Artigo

Electrochromic Behavior of Vanadium Oxide Nanostructures Synthesized by Melt Sonoquenching

de Oliveira, R. S.; Oliveira, S. C.; Alves, O. C.; Semaan, F. S.; Ponzio, E. A.*

Comportamento Eletrocrômico de Nanoestruturas de Óxido de Vanádio Sintetizadas por *Melt Sonoquenching*

Resumo: Neste trabalho um novo procedimento de síntese do V_2O_5 usando a combinação de dois métodos tradicionais, *melt quenching* e sonoquímica, chamado de *melt sonoquenching* foi proposto. O nanomaterial produzido foi caracterizado por vários métodos visando verificar características físicas e químicas, e sua possível aplicação como material eletrocrômico. Imagens de microscopia eletrônica de varredura mostraram nanofibras de óxido de vanádio com comprimentos variando de 140 a 160 nm, e diâmetros variando de 10 a 15 nm. Estudos de difração de raios X revelaram uma estrutura amorfas com espaçamento interlamelar de 13,3 Å. A composição foi estimada por TGA, sugerindo que a composição do óxido de vanádio xerogel foi de $V_2O_5.1.8H_2O$. Em adição a isto, caracterizações espectroeletroquímicas mostraram uma variação de transmitância de 45 % em 410 nm, com uma persistência de coloração de 91,3 %; tempos de resposta para oxidação e redução foram de respectivamente 1 s e 3,5 s. e a eficiência eletrocrômica foi de 55 cm^2C^{-1} ao longo de 100 ciclos de mudanças de coloração entre azul-verde-laranja.

Palavras-chave: Eletrocromismo; eletrocrômico; V_2O_5; fusão sonoresfriamento, *melt sonoquenching.*

Abstract

This paper reports a new procedure for V_2O_5 synthesis using the combination of two traditional methods, melt quenching and sonochemistry, called melt sonoquenching. The resulting nanomaterial was characterized by several methods in order to verify physical and chemical characteristics, and its possible use as electrochromic electrode material. Scanning electron micrographs revealed V_2O_5 nanofibers with lengths varying from 140 to 160 nm, and diameters varying from 10 to 15 nm, X-ray diffraction experiments pointed to an amorphous structure with an interlamellar spacing of 13.3 Å. Chemical composition was estimated by TGA, suggesting that the composition for such xerogel oxide was $V_2O_5.1.8H_2O$. Besides these, spectroelectrochemical characterization showed a transmittance variation of 45 % at 410 nm, with coloration persistence of 91.3 %, response times for the oxidation and reduction were, respectively, 1 s and 3.5 s, being such electrochomic efficiency of 55 cm^2C^{-1} in throughout 100 cycles of color changes from blue-green-orange.

Keywords: Electrochromism; electrochromic; V_2O_5; melt sonoquenching.

* Universidade Federal Fluminense, Instituto de Química, Departamento de Físico-Química, Grupo de Eletroquímica e Eletroanalítica (G2E), Outeiro de São João Batista s/nº, CEP 24020-141, Centro, Niterói-RJ, Brasil.

✉ eaponzio@vm.uff.br

Electrochromic Behavior of Vanadium Oxide Nanostructures Synthesized by Melt Sonoquenching

Renato S. de Oliveira,[a] Silvio César de Oliveira,[b] Odivaldo C. Alves,[c] Felipe S. Semaan,[d] Eduardo A. Ponzio[c,]*

[a] Instituto Federal de Educação, Ciência e Tecnologia do Rio de Janeiro, Campus São Gonçalo, Rua Dr. José Augusto Pereira dos Santos, s/nº, CEP 24425-004, Neves, São Gonçalo-RJ, Brasil.

[b] Universidade Federal de Mato Grosso do Sul, Instituto de Química, Cidade Universitária, CEP 79070-900, Campo Grande-MS, Brasil.

[c] Universidade Federal Fluminense, Instituto de Química, Departamento de Físico-Química, Grupo de Eletroquímica e Eletroanalítica (G2E), Outeiro de São João Batista s/nº CEP 24020-141, Centro, Niterói-RJ, Brasil.

[d] Universidade Federal Fluminense, Instituto de Química, Departamento de Química Analítica, Grupo de Eletroquímica e Eletroanalítica (G2E), Outeiro de São João Batista s/nº CEP 24020-141, Centro, Niterói-RJ, Brasil.

* eaponzio@vm.uff.br

1. **Introduction**

2. **Experimental**

3. **Results and Discussion**

4. **Conclusion**

1. Introduction

Electrochromic materials are a category of chromophores capable of undergo color changes by means of external electric stimulation; such great category of materials can be easily classified into different groups,[1,2] among those, one takes special place, being the class of ion insertion materials, particularly transition metals oxides.

Electrochromic transition metal oxides have been reviewed several times, being all details covered suitably in deep and range by literature, in many details in books[3,4] and reviews.[5,6] These transition metal oxides may be classified according to the color change associated to the insertion/extraction of charge as anodic or cathodic oxides.

Oxides derived from W, Mo, Nb, and Ti, have been referred as cathodic electrochromic materials, being the color changes related to charge insertions while, on the other hand, oxides from Ru, Rh, Cr, Co, Fe, Mn, Ir, and Ni have been called anodic electrochromic materials, since color changes occur as consequence of charge extractions;

according to the above given definition it is clearly noted that vanadium oxide is exception, since it presents an intermediate nature, exhibiting cathodic and anodic behaviors (presenting different colors) in different wavelength ranges and potentials.

V_2O_5 films can be promptly and reversibly converted from yellow to green by the addition of ions and even electrons, to form vanadium bronze ($M_xV_2O_5$), according to the following reaction of insertion/extraction (Eq. 1).

$$V_2O_5 \text{ (yellow)} + xM^+ + xe^- \rightleftarrows M_xV_2O_5 \text{ (green)}$$
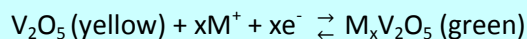
$$M = H, Li, Na \text{ or } K \text{ ions}$$

Eq. 1

Vanadium exists in many different states of oxidation (and, thus, oxide forms), di-, sesqui-, and pentoxides (VO_2, V_2O_3, and V_2O_5). They have been processed in thin film forms and applied as optical/electrical devices. In this context, vanadium oxide (V_2O_5) stands for an special case: presenting wide band gap and acting as n-type semiconductor material, such oxide form has been widely investigated due to its interesting electrochemical performance, possibilities of use in lithium secondary batteries,[7,8] and thermochromic devices.[9,10]

Electrochemical studies have shown that the performance of vanadium oxide films is directly related to their crystallinity, morphology, disorder degree, stoichiometry, and other parameters related to the methods and conditions of the synthesis. In particular, significant differences are reported, being them related to the optical transmittance of amorphous and crystalline vanadium oxide thin film electrodes under lithium electrochemical intercalation, as a consequence of external perturbation (external potential).[11] Amorphous phase is characterized by a lamellar structure which directly dependents on the amount of water present and heat treatment to which such material is subjected.[12-14] The lamellar distance plays an important role in the intercalation/mobility of ions for charge compensation during the redox processes.

Vanadium oxide can be produced by various techniques, among them we can highlight sol-gel method (method alcoxide), spray pyrolysis, magnetron sputtering, pulsed laser and/or chemical vapor deposition, electrospinning, sonochemistry, melt quenching, among others.[15-22] The synthetic paths' choice can be oriented as a function of future application, thus, such oxide can be deposited as thin films onto various substrates such as glass electrodes coated by a thin layer of ITO (tin oxide doped with indium) or even FTO (tin oxide doped with fluorine), such oxide.

Sol-gel strategy (by alcoxide) is widely used for vanadium oxide production, although some disadvantages can be easily noted, such as the use of expensive toxic precursors, long processing times and low reproducibility of properties of the final materials, only achieved through a careful control of the experimental conditions of synthesis.[23] Synthesis by sputtering also has many drawbacks, such as the use of high cost equipment, the quite low deposition rate of some materials, degradation of raw materials under high energy and pressure exposures.

Sonochemical methods have been successfully applied to the preparation of V_2O_5.[24,25] Sonochemistry rises its success in creating nanostructured materials principally from acoustic cavitation; the formation, growth, and implosive collapse of bubbles in a liquid.[26-28] On the other hand, sonochemical synthesis of different oxides can produce different crystalline structures. For example, Ohayon and col.[29] synthesized vanadium oxide by this method, reaching mixed crystalline phases, being then necessary to carry out a heat treatment after synthesis to obtain a single-phase.

The synthesis of V_2O_5 by melt-quenching,

as reported by some authors,[22,30-34] stands out due to advantages such as easy implementation and use of simpler/ cheaper equipment. Large quantities of these gels are today prepared this way for industrial purposes.

In this paper, we present a fast and easy route to produce V_2O_5 nanowires by mixing two techniques, melt-quenching, and sonochemistry; this result in a novel method called melt sonoquenching.[35] This novel synthetic route has some special advantages: low-cost, large-scale production and good electrochromic response.

2. Experimental

Amorphous vanadium pentoxide was prepared by combining melt quenching and sonochemical techniques. Suitable amounts of NH_4VO_3 (5.0 g, 99 % pure, VETEC) were melted at 800 °C in a small ceramic crucible during one hour, being then quenched by pouring the melted oxide into a Pyrex crucible with 50 mL of water, at 25 °C, placed into an active ultrasound bath (UNIQUE - USC1400, 40 kHz e 120 W). A dark red gel was obtained, being then suitably diluted providing this way a colloidal solution. The quenched material was kept in a sealed tube for 7 days. The sample was separated into two aliquots. One sample was subject to thermal treatment in a furnace at 110 °C (under air exposure) for 24 hours, and used for characterization by x-ray difractometry (Bruker-AXS-D8 advanced X-ray diffraction, 40 kV/40 mA, using monochromatized Cu kα radiation - 1.54056 Å), thermogravimetric analysis (TGA), and Infrared spectroscopy (FT-IR reflectance was recorded in the 400-4000 cm^{-1} range using a double beam spectrometer Varian 660).

Besides these, further characterization procedures were carried out by electron microscopy (MEV) and electrochemical analysis using films made by using the second separated aliquot. Fluorine doped tin oxide (FTO) (FlexiTec Organic Electronic $10 \leq R \leq 20$ Ω cm^{-1}, 42 mm^2) substrates were coated by gel-derived thin films, solvent was dried at 110°C in an air exposed furnace. Electron paramagnetic resonance (EPR) spectra were obtained at room temperature (25 °C) using a esp300e Bruker spectrometer operating at about 9.5 GHz (X band). Field emission scanning electron microscopy (FESEM) images were taken using a FEG Jeol jsm-6701f. Thermogravimetric analyzes (TGA), and differential thermal analyses (DTA) were simultaneously carried out using Shimadzu DTG-60 TGA-DTA. The fine powdered samples were placed into an opened aluminum crucibles, data were taken under 10 °C min^{-1} heat rate, from room temperature until 550 °C, under dynamic nitrogen atmosphere (50 mL min^{-1}).

Electrochemical experiments were developed by using a µAutolab III potentiostat/galvanostat, a three electrode cell was designed and prepared using as counter electrode a platinum sheet with an area of 4.5 cm^2 was used, as a quasi-reference electrode a Ag wire and, as working electrode thin films of V_2O_5 supported onto FTO substrates (42 mm^2). As supporting electrolyte solutions were prepared by adding 0.5 mol L^{-1} $LiClO_4$ (Aldrich) in pure acetonitrile (HPLC grade). A typical spectrophotometer cuvette was used as an electrochemical cell. UV-vis experiments were done by applying a Varian UV-Vis 50 spectrophotometer, in which the electrochemical cell was placed, adapting the working electrode through the optical path of the equipment.

3. Results and Discussion

In this study the V_2O_5 was obtained using the combination of two techniques, melt quenching and ultrasound exposure. Such preparation method revealed promising results strongly validating them as an alternative route for the synthesis of

nanostructures overcoming some conventional methods in terms of costs and large-scale production potential. The results obtained revealed that the ultrasound has a very important role.

The melt quenching synthesis used in the production of vanadium oxide is based on heating the vanadium oxide in temperatures above its melting point with subsequent abrupt cooling to room temperature (25 °C). The heating at 800 °C of the NH_4VO_3 for one hour was sufficient to allow the precursor to undergo total decomposition, forming vanadium pentoxide, according to reaction (Eq. 2). The melting point of the vanadium oxide occurs at a temperature of 670 °C, forming vanadium oxide in liquid state, according to reaction (Eq. 3). By putting abruptly the liquid vanadium oxide into water under ultrasonic bath at room temperature, a gel is immediately formed ($V_2O_5.nH_2O$ xerogel) with a dark orange color, according to reaction (Eq. 4).

$$2\ NH_4VO_{3\ (s)} \xrightarrow{\Delta} V_2O_{5\ (s)} + 2\ NH_{3\ (g)} + H_2O_{\ (g)} \tag{2}$$

$$V_2O_{5\ (s)} \xrightarrow{800°C} V_2O_{5\ (l)} \tag{3}$$

$$V_2O_{5\ (l)} + n\ H_2O_{\ (l)} \xrightarrow{T_{amb}} V_2O_5.n\ H_2O_{\ (gel)} \tag{4}$$
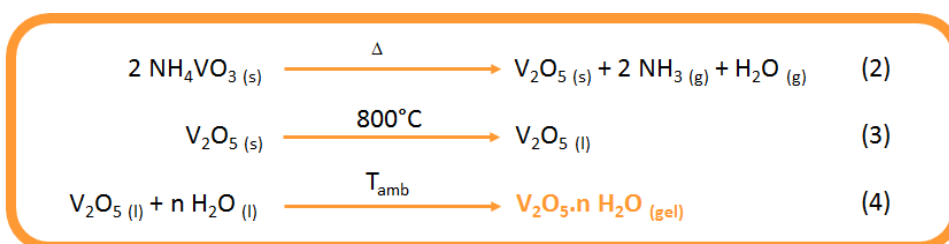
The influence of ultrasonic radiation over heterogeneous media is complex since it may involve several chemical and/or physical processes, such as the production of reactive free radicals, shock waves, mass transfer, microstreaming, microjets, enormous local temperatures and pressures, mixing, etc., all associated with the process of cavitation.[36]

Currently, the influence of ultrasound waves and the mechanism of formation of the V_2O_5 are still under investigation. The reactions were induced by low frequency/high intensity sound waves, resulting in a more violent cavitation bubble, generating a higher localized temperature and pressure, what could, possibly, improve the formation of nanostructures of V_2O_5.

Apparently, physical effects such as microstreaming, microstreamers, microjets, and shock waves cause turbulent fluid movements and provoke, during the cooling process, a unique crystal growth. The fast uniform cooling process creates a kinetic condition unfavorable to the occurrence of recrystallization but favorable to produced nanowires. The microstreaming in association to the microjets results in desaggregation of particles, erosion on particle's surface and prevent the particle growth.

Radical species may react with the material surface; however, due to the short treatment periods in this study, radicals were not expected to have an effect on the system.

Figure 1 presents the results of the X-ray diffractometry (XRD), in which the XRD pattern reveals the formation of an amorphous material. The presence of diffraction peak in $2\theta = 6.6°$ referring to the diffraction plan (001) corresponds to an interllamelar spacing of approximately 13.3 Å, there is still another peak in $2\theta = 25.5°$ referring to diffraction plan (003). These results are in accordance to those found in literature for $V_2O_5.nH_2O$ xerogel.[12]
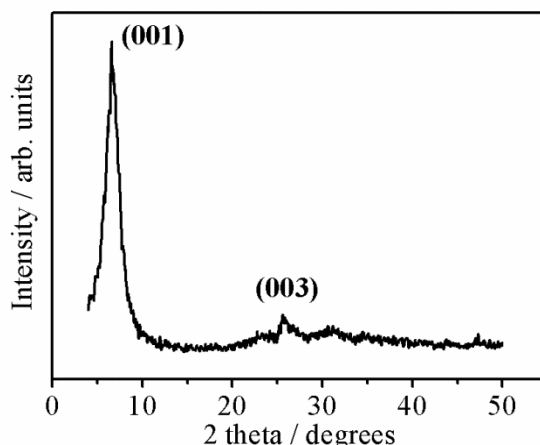
Figure 1. X-ray diffractometry (XRD) pattern of V_2O_5 xerogel

The interllamelar spacing of 13.3 Å corresponds to the distance between the vanadium oxide lamellas separated by water molecules. With the intention of verifying the relation between the interllamelar spacing and the quantity of intercalated water, measurements were made of TGA-DTA, according to Figure 2.
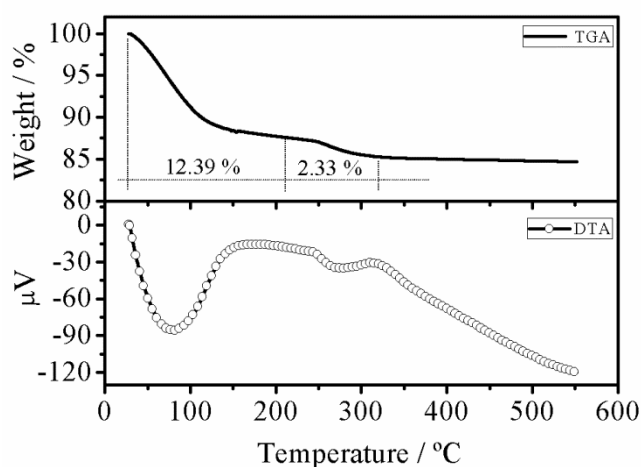
Figure 2. TGA-DTA measurements of V_2O_5 xerogel

Thermogravimetric analysis showed in Figure 2(a) presents two well defined stages of mass loss. The first, with a mass loss of 12.39 %, is attributed to the loss of water adsorbed between the lamellas of vanadium oxide extending up to 210 °C; the second stage, on the other hand, had lower intensity (2.33 % of mass loss), and could be observed between 210 and 320 °C, such event is possibly related to the release of water molecules coordinated to the vanadyl groups, and molecules present in the lamella plan.[37] Considering that the initial mass of the sample was 11.3617 mg, by a simple mathematical relation, it was determined that the mass of water present in the V_2O_5 dry gel was 1.6724 mg, that is, 1.8 mol of water per mol of V_2O_5, therefore the most

probable formula of hydrated vanadium oxide is $V_2O_5.1.8H_2O$.

The formula $V_2O_5.1.8H_2O$ is directly related with the interplanar distance of 13.3 Å. Comparing the data of the hydrated vanadium oxide structure and the interllamelar spacing, it can be noted that they are coherent with the data found in literature according to Table 1.

Table 1. Composition and interlayer distance (d) of $V_2O_5.nH_2O$ according to literature

Composition	d (Å)	Literature
$V_2O_5.0,5H_2O$	8,7	Baddour *et al.*[38]
$V_2O_5.1,6H_2O$	11,6	Zakharova *et al.*[13]
$V_2O_5.nH_2O$ (n = 1,6 - 1,8)	11,8	Kang *et al.*[14]
$V_2O_5.1,9H_2O$	11,8	Oliveira *et al.*[37]

It was also noted that as the quantity of intercalated water increases, the interllamelar spacing increases; and that the values of interplanar distance for similar structure is viable, but oscillates near the same value, which is probably related to different drying times of the synthesized materials, and also due to the different synthesis methods applied.

The morphology of the vanadium oxide was analyzed using a field emission scanning electron microscopy (FEG-SEM), according to Figure 3. The presence of a nanofibrous structure can be seen composed by agglomerates of fibers of V_2O_5 with lengths varying from 140 to 160 nm and diameters varying from 10 to 15 nm.
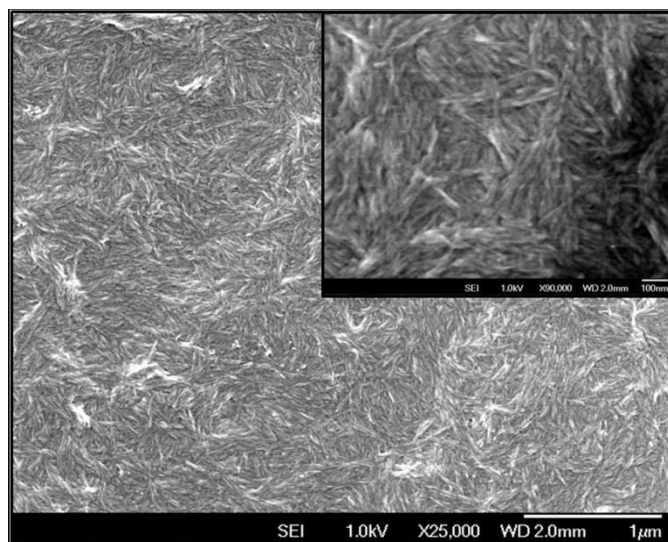
Figure 3. Field emission scanning electron microscopy (FEG-SEM) of V_2O_5 nanowires (x25.000). Inside micrograph of V_2O_5 with magnification of x90.000

Several articles have reported the synthesis of V_2O_5 by thermal decomposition of NH_4VO_3 and the melting quenching of V_2O_5. When V_2O_5 is prepared by thermal decomposition of NH_4VO_3 the synthesis results in powdered materials with particle size of few micrometers.[39-43]

For example, Adhikary and col.[30] obtained V_2O_5 fibers from a melt quenching with a size from 2 to 3 mm in length and 0.1 mm in width; Cocciantelli and col.[34] observed different sizes varying from 2 up to 50 um.

For other hand, Livage and col.[42] produced amorphous V_2O_5 by the splat cooling of the molten oxide and this oxide made of cross-linked fibers about some micrometer long.

Sizes of particles seen in the mixed synthesis is related to the fact that in the melt quenching synthesis the process of fast cooling. The use of the ultrasonic bath in the synthesis of V_2O_5 provides a higher homogenization of the medium and contributes to the increase of cooling rate, which causes a decrease in the growth of crystals. Therefore, this type of synthesis provides the formation of stable nanoparticles.

The hydrated vanadium oxide was also characterized by infrared spectroscopy (Figure 4), in which were observed a band at 998 cm^{-1} assigned to the distention of groups V=O not equivalent, a band at 798 cm^{-1} related to the distention of connection V-O, and a band at 532 cm^{-1} assigned to the asymmetric distention of V-O-V, all of these designations are in accordance to the data found in literature.[13,44]
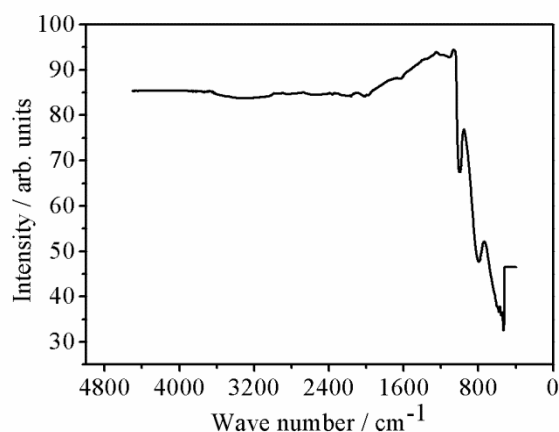
Figure 4. FT-IR spectrum of V_2O_5 xerogel

Another way to characterize the materials is using electron paramagnetic resonance (EPR) spectroscopy. As shown in Figure 5 the EPR spectrum recorded at room temperature can be fitted by the sum of two components indicating that the ions V^{4+} is not distributed homogeneously, with regions of different ionic densities.

The component A at g = 1.97 is broad (line with of 100 G) and structure less displaying a symmetric line shape. The absence of hyperfine interaction indicates strong interaction between the ions V^{4+}.[45,46]

The second component shows the typical liquid-like isotropic spectrum, consisting of eight lines due to hyperfine interaction of the unpaired electron with ^{51}V whose natural abundance is 99.5 % and nuclear spin is I = 7/2.

The simulations using easy-spin program[47] yield g-values and hyperfine components $g_0 = 1,97$ and $A_0 = 116\,G$ that seemed to be in good agreement with those obtained for the high temperature liquid-like spectrum of vanadium pentoxide gel.
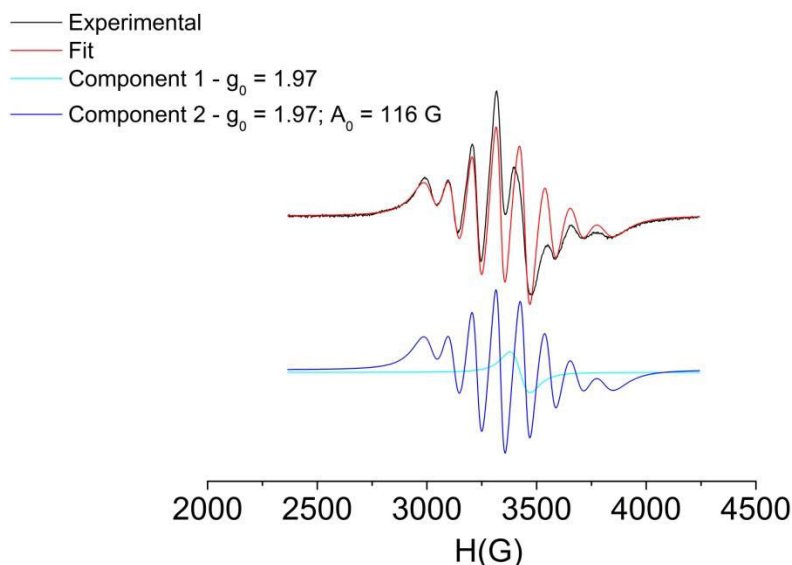
Figure 5. Electron paramagnetic resonance (EPR) spectroscopy of V_2O_5 xerogel

This isotropic spectrum confirms the formation of an amorphous material obtained by XRD and is due to Brownian motion of paramagnetic species on the surface. This molecular motion is only possible due to the presence intercalation water that provides enough interlayer space for vanadyl ions to move.

Spectroelectrochemical characterization in situ of the synthesized vanadium oxide was made in order to verify their potentialities for application in electrochromic electrodes. A fundamental characteristic for the application in electrodes of electrochromic devices is the reversibility in the redox and concomitant process of intercalation/deintercalation of ions in the electrode's structure.

The results of cyclic voltammetry experiments for V_2O_5, Figure 6(a) shows with the applied voltage was between -0.6 and 1.2 V relative to Ag quasi-reference electrode with a scanning rate of 5 mV s^{-1} and Pt was used as a counter electrode in electrolyte (0.5 mol L^{-1} LiClO$_4$/acetonitrile), revealed a reversibility of the redox processes. In the direct sweep, when analyzing the chart in Figure 6(a) it is possible to observe the presence of two oxidation waves, one at 0.18 V and another at 0.60 V. The first is due to the oxidation of part of the vanadium sites (+4) to vanadium (+5). The second oxidation wave corresponds to the oxidation in the remaining vanadium sites (+4) for the state of oxidation +5. During the inverse sweep, it is also possible to observe the occurrence of two peaks of reduction, one at 0.42 V related to the reduction of part of V (+5) to V (+4) and another at -0.27 V related to the reduction of other vanadium sites (+4).

Figure 6(b) shows two UV-Vis spectra obtained with the chronoamperometry technique, in which we applied the extremes potentials used in the cyclic voltammetry technique. The conjoint analysis of the cyclic voltammetry (Figure 6(a)) with the UV-Vis spectra (Figure 6(b)) shows that at the end of the oxidation stage of the material, at 1.2 V, the same has an absorption band at 378 nm. It was also observed that in the beginning of the anodic sweep at -0.6 V, an accentuated decrease of the band situated at 378 nm and the appearance of a lower intensity band at 748 nm.
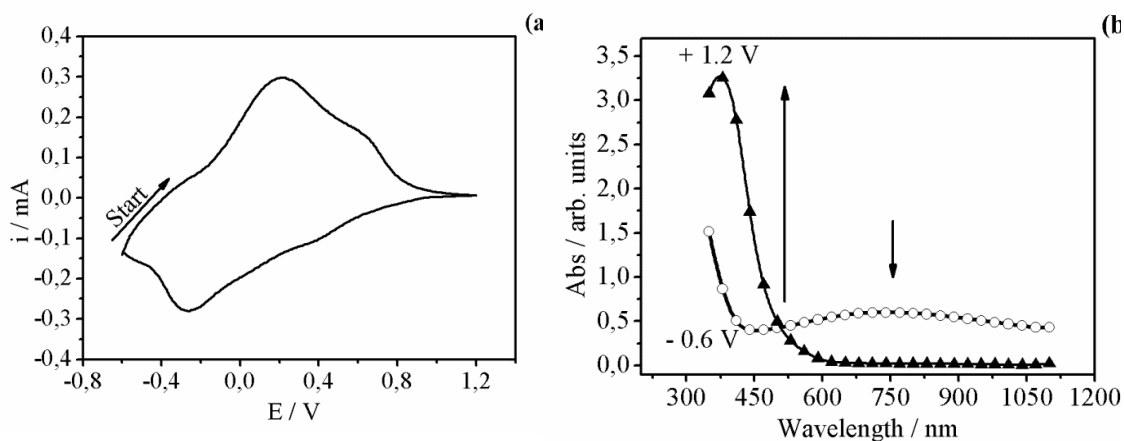
Figure 6. Cyclic voltammetry experiments in (a) and UV-Vis spectra in (b) for V_2O_5 produced

When observing if the behavior of the absorption spectra of the material due to the applied potential, imposing 1.2 V, only one band is seen with the maximum absorption at 378 mm. This band corresponds to a transition by load transference for the V (+5), in which according to Ryczkowsky[48] the load transference of the binder to the metal (LMTC) occur in regions from 200 to 550 nm. In another study, Chary and col.,[49] indicated that the band at approximately 380 nm refers to the transition that occurs from the binder to the metal (LMTC) typical of ions V (+5) coordinated by five oxygen atoms in the shape of a square-based pyramid. When applying -0.6 V, the spectrum obtained show

a wide band at 748 nm, which corresponds to transition d-d that occurs for V (+4) in the region 400-1000 nm and has a very low intensity when compared to the LMTC transitions.

The wavelength in which the V_2O_5 has the highest absorbance variation (Figure 6(b)) is 410 nm, thus, we made a follow-up of the change in color in the V_2O_5 through cyclic voltammetry experiments in this length of specific wave. Figure 7 presents the results of the measurements *in situ* of cyclic voltammetry and transmittance variation in function of the potential in the wavelength of 410 nm for the V_2O_5.
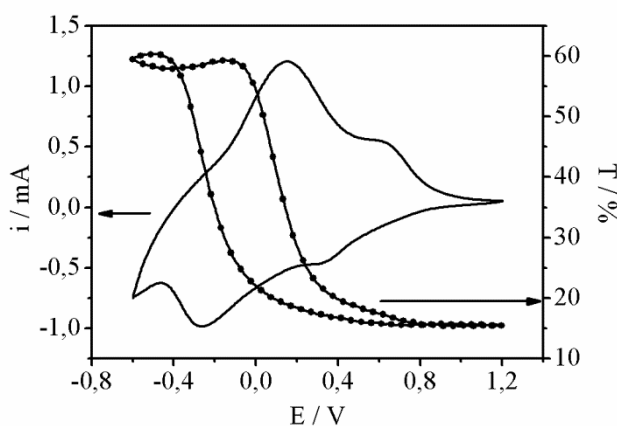
Figure 7. Cyclic voltammetry and transmittance variation *in situ* in function of the potential in the wavelength of 410 nm for the V_2O_5

Transmittance variation of circa 45 % (410 nm) has been noted. This indicates that the material modulates its color in function of a difference of potential applied, allowing and encouraging its use for application in electrochromic devices.

With the intention of proving the existence of a direct cause/effect relationship between applied potential and variations in optic properties of V_2O_5 at 410 nm, the derivative of absorbance variation related to time in function of the potential range was calculated. Figure 8 shows a cyclic voltammogram along with the absorbance derivative in function of time.

The methods came from the principle that in electrochemical processes the absorbance variation are proportional to the electric charges involved, therefore, the maximums and minimums obtained by the absorbance differentiation in relation to time (dA/dt) must correspond to the oxidation-reduction peaks seen in cyclic voltammogram, except if the capacitive current does not show in the optic measurement. In wavelength values in which curves dA/dt and i *vs* E coincide, species involved in the redox reactions are responsible for the color alteration in the studied wavelength.

Figure 8 shows that the potential peaks of anodic and cathodic currents of the voltammograms coincide with the maximum and minimum of the dA/dt curves for the measurements made at 410 nm, which indicates that the transference of electrons occurred in these processes generating, this way, color changes.
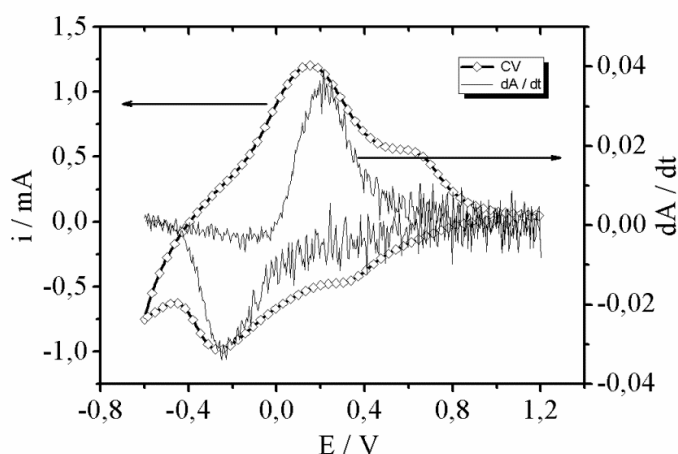
Figure 8. Cyclic voltammogram and absorbance differentiation in relation to time (dA/dt in 410 nm) in situ for the V_2O_5 produced

The absorbance derivative as function of time showed that for an infinitesimal variation of absorbance in potential range from -0.6 to 1.2 V, it is possible to observe that oxidizing the material at approximately 0.2 V causes a decrease in transmittance. This indicates that the material is absorbing the wavelength radiation of 410 nm, taking a positive variation of dA/dt soon after completing oxidation according to Figure 8. Under a potential of approximately -0.35 V, during the reduction stage, we noticed an increase in transmittance favoring the passage of wavelength radiation of 410 nm. In this moment, there is a negative variation of dA/dt. Considering this, it can be verified that the process of change in spectrum is directly related to the electrochemical process of oxidation and reduction.

Aiming to assess the behavior of the electrode in several cycles of oxidation and reduction, followed by the absorbance variations during these processes,

chronoamperometric analysis were carried out monitoring optic density variations in situ. Using the wavelength of 410 nm, successive programmed cycles (potentials of -0.6 V for 10 seconds, and 1.2 V for the same duration) were applied. Changes of color from blue to orange were monitored as a function of cycling time. Figure 9 (a) and (b)

show, after 100 cycles of color changes the material's transmittance variations keep a practically constant behavior, around 91.3 % of the initial variation. It can also be observed that application time intervals of the used potentials (10 seconds) were suitable and sufficient to promote the color changes among blue, green and orange.
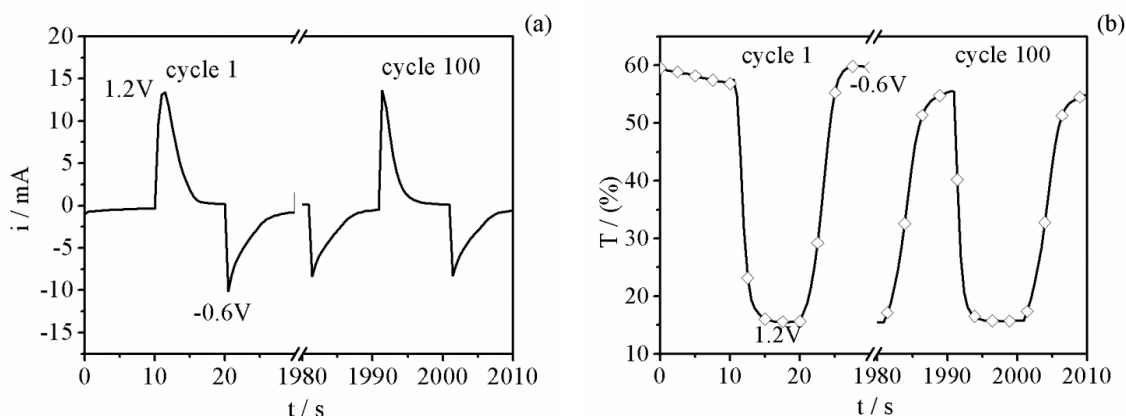
Figure 9. Chronoamperometric analysis was with in situ optic density variation using the wavelength of 410 nm

With the data obtained in Figure 9, the electrochromic efficiencies and the response times were calculated for the oxidation and reduction of V_2O_5.

The electrochromic efficiency relates the absorbance variation (ΔA) with the inserted charge per unit of film area (Q) in the system. It is calculated using the integration of current curve versus time (figure 9(a)). The electrochromic efficiency (η) is defined according to the Equation 5 below.

$$\eta = \Delta A/Q \qquad \text{Eq. 5}$$

We have noticed that for the reduction as well as the oxidation of the vanadium oxide as the 100 cycles are made, the electrochromic efficiency of V_2O_5 kept at 55 cm^{2}C^{-1} (410 nm).

The electrochromic response time (t) is the necessary time for the material to change color, although there is not specific criterion to determine this response time, it could have been obtained by the total transmittance variation (or absorbance) or by a fraction of this.[50] In this study, the response time calculation is defined as the necessary time from the beginning of the pulse until it reaches 50 % of the total transmittance or absorbance variation of each pulse. The response times are presented in Figure 10.

In analyzing the response times necessary for the oxidation and reduction of the material a significant difference between them can be noticed. The response time of the reduction (around 3.5 seconds) is always higher than the response time for the oxidation (less than 1 second) throughout the 100 cycles, indicating that the V_2O_5 film takes a time approximately 3.5 times longer to become blue than to become orange.
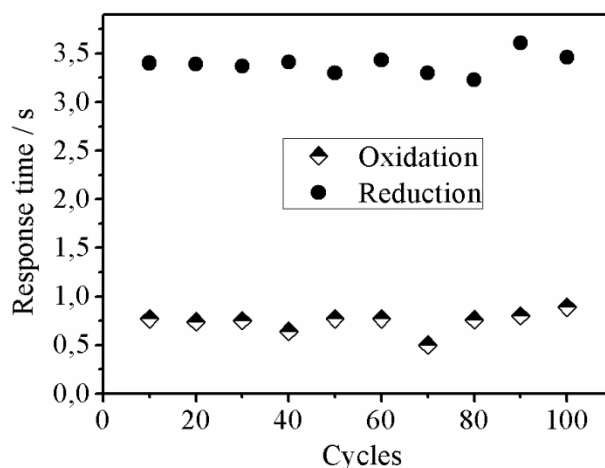
Figure 10. Electrochromic response time of V_2O_5

Another important parameter is the coulombic efficiency, given by the oxidation/reduction charges ratio, it was noticed for the first cycle of oxidation-reduction the coulombic efficiency was 1.27 showing that during the first cycle the process of oxidation was more effective than the reduction of the material and consequently, the de-insertion of the lithium ions is more effective than the insertion of Li^+ ions in the structure of V_2O_5. On the 100th cycle the coulombic efficiency was 0.98 indicating that the oxidation charge is practically balanced with the reduction. Therefore, with every cycle, there was stabilization in the flow of Li^+ ions in the material in order that in this cycle the insertion and de-insertion of Li^+ ions are practically the same.

Table 2 shows some important electrochromic parameters in scientific literature. In comparing this data with the ones obtained for vanadium oxide in this study, we can see that the electrochromic efficiency values found here are higher than the ones found in literature. In relation to the response times and transmittance variation, the values obtained are comparable, and in some cases even better than the ones found in literature.

Table 2. Comparison of electrochromic efficiency values, response times, transmittance variation and wavelengths found in literature to the ones found in this study

η $(cm^2 C^{-1})$	Response time (s)	ΔT (%)	Wavelength nm	Literature
~ 55	~3.5 e ~1	45	410	**This work**
14	2	------	800	Nagase *et al.*[51]
------	6 e 5	37,4	415	Cheng *et al.*[52]
13	-------	-------	630	Patil *et al.*[53]
33.7	-------	36,5	400	Lin *et al.*[54]
-------	6 e 1	60	633	Xiong *et al.*[55]

This is due to the increase of specific superficial area, which reduces significantly the diffusion pathway of the Li^+ ions, and simultaneously, the number of accessible intercalation sites. This effect improved kinetics transport for electrochemical intercalation.

4. Conclusion

The synthesized lamellar vanadium oxide through a combination of synthesis, melt quenching and sonochemistry presented an interllamelar spacing of 13.3 Å. Its composition was estimated by TGA, which showed that the structure of the xerogel oxide was $V_2O_5 \cdot 1.8H_2O$. The FESEM images proved the presence of a fibrous structure comprised by agglomerates of fibers of V_2O_5 with lengths varying from 140 to 160 nm, and diameters varying from 10 to 15 nm. The hydrated vanadium oxide was also characterized by FT-IR and EPR which proved its synthesis. The use of this oxide in electrochromic electrodes, through spectroelectrochemical measurements *in situ* showed a transmittance variation of 45 % in a wavelength of (410 nm) maintaining color at around 91.3 % after 100 cycles; response times for the oxidation and reduction were below 3.5 seconds, electrochromic efficiency of approximately 55 cm^2 C^{-1} at 410 nm throughout the 100 cycles of color change among blue-green-orange. The values of coulombic efficiency indicated that within each cycle there was a stabilization of the material in order that in the 100th cycle the insertion and de-insertion of Li^+ ions are practically the same. All of the verified electrochromic parameters showed that this oxide has great potential for the application in electrochromic electrodes.

Acknowledgments

References

[1] Donnadieu, A. Electrochromic materials. *Materials Science and Engineering: B* **1989**, *3*, 185. [CrossRef]

[2] Oliveira, R. S.; Semaan, F. S; Ponzio, E. A. Janelas Eletrocrômicas: Uma Nova Era em Eficiência Energética. *Revista Virtual de Química* **2015**, *7*, 336. [CrossRef]

[3] Oliveira, M. R. S.; Mello, D. A. A.; Oliveira, R. S.; Ponzio, E. A.; Oliveira, S. C. In *Advances in Nanotechnology*; Bartul, Z.; Trenor, J., eds.; Nova Publishers: New York, 2011, Vol 8, cap. 1. [Link]

[4] Monk, P. M. S.; Mortimer, R. J.; Rosseinsky, D. R. *In Electrochromism: Principles and Applications*; Bernd Speiser, ed.; VCH Verlagsgesellschaft: Weinheim, 1995; Vol 108, cap. 3. [CrossRef]

[5] Granqvist, C. G.; Niklasson, G. A.; Azens, A. Electrochromics: Fundamentals and energy-related applications of oxide-based device. *Applied Physics A* **2007**, *89*, 29. [CrossRef]

[6] Granqvist, C. G.; Azens, A.; Smulko, J.; Kish, L. B. Oxide-based electrochromics for energy efficient buildings: materials, technologies, testing, and perspectives. *Journal of Physics: Conference Series* **2007**, *93*, 012021. [CrossRef]

[7] Ponzio, E. A.; Benedetti, T. M.; Torresi, R. M. Electrochemical and morphological stabilization of V_2O_5 nanofibers by the

addition of polyaniline. *Electrochimica Acta* **2007**, *52*, 4419. [CrossRef]

8 Livage, J. Sol-gel chemistry and electrochemical properties of vanadium oxide gels. *Solid State Ionics* **1996**, *86-88*, 935. [CrossRef]

9 Granqvist, C. G.; Green, S.; Niklasson, G. A.; Mlyuka, N. R.; von Kraemer, S.; Georen, P. Advances in chromogenic materials and devices. *Thin Solid Films* **2010**, *518*, 3046. [CrossRef]

10 Granqvist, C. G.; Lansaker, P. C.; Mlyuka, N. R.; Niklasson, G. A.; Avendano, E. Progress in chromogenics: New results for electrochromic and thermochromic materials and devices. *Solar Energy Materials and Solar Cells* **2009**, *93*, 2032. [CrossRef]

11 Scarminio, J.; Talledo, A.; Andersson, A. A.; Passerini, S.; Decker, F. Stress and electrochromism induced by Li insertion in crystalline and amorphous V_2O_5 thin film electrodes. *Electrochimica Acta* **1993**, *38*, 1637. [CrossRef]

12 Pyun, S.-I.; Bae, J.-S. Electrochemical lithium intercalation into vanadium pentoxide xerogel film electrode. *Journal of Power Sources* **1997**, *68*, 669. [CrossRef]

13 Zakharova, G. S.; Volkov, V. L. Intercalation compounds based on vanadium(V) oxide xerogel. *Russian Chemical Reviews* **2003**, *72*, 311. [CrossRef]

14 Kang, S.-G.; Kim, K. M.; Park, N.-G.; Ryu, K. S.; Chang, S.-H. Factors affecting the electrochemical performance of organic/V_2O_5 hybrid cathode materials. *Journal of Power Sources* **2004**, *133*, 263. [CrossRef]

15 Benmoussa, M.; Outzourhit, A.; Bennouna, A.; Ihlal, A. Li^+ ions diffusion into sol-gel V_2O_5 thin films: electrochromic properties. *European Physical Journal: Applied Physics* **2009**, *48*, 10502. [CrossRef]

16 Patil, C. E.; Jadhav, P. R.; Tarwal, N. L.; Deshmukh, H. P.; Karanjkar, M. M.; Patil, P. S. Electrochromic performance of mixed V_2O_5–MoO_3 thin films synthesized by pulsed spray pyrolysis technique. *Materials Chemistry and Physics* **2011**, *126*, 711. [CrossRef]

17 Zou, C. W.; Yan, X. D.; Chen, R. Q.; Wu, Z. Y.; Alyamani, A.; Gao, W. Effect of annealing on the microstructure and optical properties of ZnO/V_2O_5 composite. *Applied Physics Letters* **2011**, *98*, 111904. [CrossRef]

18 Iida, Y.; Kaneko, Y.; Kanno, Y. Fabrication of pulsed-laser deposited V_2O_5 thin films for electrochromic devices. *Journal of Materials Processing Technology* **2008**, *197*, 261. [CrossRef]

19 Nandakumar, N. K.; Seebauer, E. G. Low temperature chemical vapor deposition of nanocrystalline V_2O_5 thin films. *Thin Solid Films* **2011**, *519*, 3663. [CrossRef]

20 Yu, D.; Chen, C.; Xie, S.; Liu, Y.; Park, K.; Zhou, X.; Zhang, Q.; Li, J.; Cao, G. Mesoporous vanadium pentoxide nanofibers with significantly enhanced Li-ion storage properties by electrospinning. *Energy & Environmental Science* **2011**, *4*, 858. [CrossRef]

21 Mao, C.-J.; Pan, H.-C.; Wu, X.-C.; Zhu, J.-J.; Chen, H.-Y. Sonochemical Route for Self-Assembled V_2O_5 Bundles with Spindle-like Morphology and Their Novel Application in Serum Albumin Sensing. *The Journal of Physical Chemistry B* **2006**, *110*, 14709. [CrossRef]

22 Zhang, Y.; Hu, X.; Liu, Y.; Gu, Q.; Cheng, Y. Process Parameters of A-V_2O_5 Prepared by melt-quenching method. *Electrochemical and Solid-State Letters* **2005**, *8*, A646. [CrossRef]

23 Collinson, M. M. Sol-Gel Strategies for the preparation of selective materials for chemical analysis. *Critical Reviews in Analytical Chemistry* **1999**, *29*, 289. [CrossRef]

24 Taufiq-Yap, Y. H.; Wong, Y. C.; Zainal, Z.; Hussein, M. Z. Synthesis of self-assembled nanorod vanadium oxide bundles by sonochemical treatment. *Journal of Natural Gas Chemistry* **2009**, *18*, 312. [CrossRef]

25 Mao, C.-J.; Pan, H.-C.; Wu, X.-C.; Zhu, J.-J.; Chen, H.-Y. Sonochemical Route for Self-Assembled V_2O_5 Bundles with Spindle-like

Morphology and Their Novel Application in Serum Albumin Sensing. *The Journal of Physical Chemistry B* **2006**, *110*, 14709. [CrossRef]

26 Gedanken, A. Using sonochemistry for the fabrication of nanomaterials. *Ultrasonics Sonochemistry* **2004**, *11*, 47. [CrossRef]

27 Bang, J. H.; Suslick, K. S. Applications of Ultrasound to the Synthesis of Nanostructured Materials. *Advanced Materials* **2010**, *22*, 1039. [CrossRef]

28 Zhang, Y.; Lin, S.; Fang, Y. New developments in sonochemistry, preparation of nanomaterials by ultrasound. *Chinese Physics Letters* **2002**, *31*, 80. [Link]

29 Ohayon, E.; Gedanken, A. The application of ultrasound radiation to the synthesis of nanocrystalline metal oxide in a non-aqueous solvent. *Ultrasonics Sonochemistry* **2010**, *17*, 173. [CrossRef]

30 Adhikary, K.; Kikkawa, S. Preparation and electrochemical lithium intercalation of V_2O_5 porous lump with large surface area1. *Solid State Ionics* **1997**, *99*, 53. [CrossRef]

31 Nabavi, M.; Sanchez, C.; Taulelle, F.; Livage, J.; Guibert, A. Electrochemical properties of amorphous V_2O_5. *Solid State Ionics* **1988**, *28-30*, 1183. [CrossRef]

32 Livage, J.; Collongues, R. Semiconducting properties of amorphous V_2O_5 prepared by splat cooling. *Materials Science and Engineering* **1976**, *23*, 297. [CrossRef]

33 Livage, J.; Gharbi, N.; Leroy, M. C.; Michaud, M. Hydratation et texture fibreuse de V_2O_5 amorphe. *Materials Research Bulletin* **1978**, *13*, 1117. [CrossRef]

34 Cocciantelli, J. M.; Ménétrier, M.; Delmas, C.; Doumerc, J. P.; Pouchard, M.; Broussely, M.; Labat, J. On the δ → γ irreversible transformation in $Li//V_2O_5$ secondary batteries. *Solid State Ionics* **1995**, *78*, 143. [CrossRef]

35 de Oliveira, R. S.; da S. Goulart, J.; Miranda, F. S.; Ponzio, E. A. Melt sonoquenching: an affective process to obtain new hybrid material and achieve enhanced electrochromic performances based on V_2O_5 /2,4,5-tris(1-methyl-4-pyridinium)-imidazolide tetrafluoroborate nanofibers. *Journal of the Brazilian Chemical Society* **2014**, *25*, 540. [CrossRef]

36 Klima, J. Application of ultrasound in electrochemistry. An overview of mechanisms and design of experimental arrangement. *Ultrasonics* **2011**, *51*, 202. [CrossRef]

37 Oliveira, H. P.; Graeff, C. F. O.; Rosolen, J. M. Synthesis and structural characterization of tetrakis(n-methyl-4-pyridyl) porphyrin copper into V_2O_5 xerogel. *Materials Research Bulletin* **1999**, *34*, 1891. [CrossRef]

38 Baddour, R.; Pereira-Ramos, J. P.; Messina, R.; Perichon, J. A thermodynamic, structural and kinetic study of the electrochemical lithium intercalation into the xerogel V_2O_5.1.6 H_2O in a propylene. *Journal of Electroanalytical Chemistry and Interfacial Electrochemistry* **1991**, *314*, 81. [CrossRef]

39 Shimizu, A.; Tsumura, T.; Inagaki, M. Electrochemical intercalation of lithium into V_2O_5: Effect of host materials. *Solid State Ionics* **1993**, *63-65*, 479. [CrossRef]

40 Murphy, D. W.; Christian, P. A.; DiSalvo, F. J.; Carides, J. N.; Waszczak, J. V. Lithium incorporation by V_6O_{13} and related vanadium (+4, +5) oxide cathode materials. *Journal of The Electrochemical Society* **1981**, *128*, 2053. [CrossRef]

41 Dickens, P. G.; Reynolds, G. J. Transport and equilibrium properties of some oxide insertion compounds. *Solid State Ionics* **1981**, *5*, 331. [CrossRef]

42 Gharbi, N.; R'Kha, C.; Ballutaud, D.; Michaud, M.; Livage, J.; Audiere, J. P.; Schiffmacher, G. A new vanadium pentoxide amorphous phase. *Journal of Non-Crystalline Solids* **1981**, *46*, 247. [CrossRef]

43 Takiyama, K. Formation and Aging of Precipitates. VI. Morphology of Crystals in Various Vanadium Pentoxide Sols by Electron Microscopy. *Bulletin of the Chemical Society of Japan* **1958**, *31*, 329. [CrossRef]

44 Somani, P. R.; Marimuthu, R.; Mandale, A. B. Synthesis, characterization and charge transport mechanism in conducting polyaniline/V$_2$O$_5$ composites. *Polymer* **2001**, *42*, 2991. [CrossRef]

45 Narayana, K. V.; Raju, B. D.; Masthan, S. K.; Rao, V. V.; Rao, P. K.; Subrahmanian, R.; Martin, A. ESR spectroscopic characterization of V$_2$O$_5$/AlF$_3$ ammoxidation catalysts. *Catalysis Communications* **2004**, *5*, 457. [CrossRef]

46 Nascimento, O. R.; Magon, C. J.; Lima, J. F.; Donoso, J. P.; Benavente, E.; Paez, J.; Lavayen, V.; Santa, A. M. A.; Gonzalez, G. Magnetic resonance study of a vanadium pentoxide gel. *Journal of Sol-Gel Science and Technology* **2008**, *45*, 195. [CrossRef]

47 Stoll, S.; Schweiger, A. EasySpin, a comprehensive software package for spectral simulation and analysis in EPR. *Journal of Magnetic Resonance* **2006**, *178*, 42. [CrossRef]

48 Ryczkowsky, J. IR spectroscopy in catalysis. *Catalysis Today* **2001**, *68* 263. [CrossRef]

49 Liu, J.; Zhao, Z.; Xu, C.; Duan, A.; Zhu, L.; Wang, X. The structures of VO$_x$/MO$_x$ and alkali-VO$_x$/MO$_x$ catalysts and their catalytic performances for soot combustion. *Catalysis Today* **2006**, *118*, 315. [CrossRef]

50 Chary, K. V. R.; Kumar, C. P.; Naresh, D.; Bhaskar, T.; Sakata, Y. Characterization and reactivity of Al$_2$O$_3$-ZrO$_2$ supported vanadium oxide catalysts. *Journal of Molecular Catalysis A: Chemical* **2006**, *243*, 149. [CrossRef]

51 Vidotti, M.; Torresi, R. M.; Torresi, S.I.C. Eletrodos modificados por hidróxido de níquel: um estudo de revisão sobre suas propriedades estruturais e eletroquímicas visando suas aplicações em eletrocatálise, eletrocromismo e baterias secundárias. *Química Nova* **2010**, *33*, 2176. [CrossRef]

52 Nagase, K.; Shimizu, Y.; Miura, N.; Yamazoe, N. Electrochromic properties of vanadium pentoxide thin films prepared by new wet process. *Applied Physics Letters* **1992**, *60*, 802. [CrossRef]

53 Cheng, K.-C.; Chen, F.-R.; Kai, J.-J. V$_2$O$_5$ nanowires as a functional material for electrochromic device. *Solar Energy Materials and Solar Cells* **2006**, *90*, 1156. [CrossRef]

54 Patil, C. E.; Tarwal, N. L.; Shinde, P. S.; Deshmukh, H. P.; Patil, P. S. Synthesis of electrochromic vanadium oxide by pulsed spray pyrolysis technique and its properties. *Journal of Physics D: Applied Physics* **2009**, *42*, 1. [CrossRef]

55 Lin, Y.-S.; Tsai, C.-W. Reactive sputtering deposition of V$_2$O$_{5-z}$ on flexible PET/ITO substrates for electrochromic devices. *Surface and Coatings Technology* **2008**, *202*, 5641. [CrossRef]